

Power quality improvement using PV fed series active power filter with enhanced Jaya optimized PI controller

Ravikanth Mallajoshula, I. E. S. Naidu

Department of Electrical, Electronics and Communication Engineering, GITAM (Deemed to be University), Visakhapatnam, India

Article Info

Article history:

Received Nov 23, 2023

Revised May 24, 2024

Accepted Jun 2, 2024

Keywords:

Enhanced Jaya
Harmonics
Hysteresis
ICC-technic
Power quality
PV-fed SAF
THD

ABSTRACT

In this paper, improvement of power quality (PQ) in a distribution system using a PV-series active power filter (PV-SAPF) investigated. The performance of the proposed filter is increased using an enhanced Jaya optimized proportional integral (PI) with indirect current controller (ICC) technique system. In existing Jaya optimization technique best and worst cases were obtained from the whole solutions which degrades the output of the PI controller results more iteration. In case of enhanced Jaya, the proposed one, population from best to worst is sorted first and divide them as two groups best and worst solutions. The best solution is chosen from the best solution group as "Best," and the best solution from the worst solution group is chosen as "Worst". This procedure decreases the number of iterations needed to reach the optimal solution. The effectiveness of the enhanced Jaya optimization and ICC developed controller is implemented in the proposed PV-SAPF. To proof its effectiveness different types of loads are taken as case study. MATLAB/Simulink platform is used to do the above research work.

This is an open access article under the [CC BY-SA](https://creativecommons.org/licenses/by-sa/4.0/) license.



Corresponding Author:

Ravikanth Mallajoshula

Department of Electrical, Electronics and Communication Engineering, GITAM (Deemed to be University)

Visakhapatnam, Andhra Pradesh 530045, India

Email: ravikant235@gmail.com

NOMENCLATURE

R_s	: Source resistance of system	I_{sm}	: Peak current
L_s	: Source inductance of system	U_a, U_b, U_c	: Unit templates
R_f	: Resistance between inverter and grid	$i_{sa}^*, i_{sb}^*, i_{sc}^*$: Reference currents
L_f	: Inductance between inverter and grid	L_b, U_b	: Lower bound, upper bound
i_{La}, i_{Lb}, i_{Lc}	: Load currents	k_p, k_i	: Proportional, integral gain
$I_{sam}, I_{sbm}, I_{scm}$: Real components	J, MSE	: Optimization, mean square error

1. INTRODUCTION

The growing utilization of non-symmetric based loads in distribution network leads to a significant rise in various voltage and current related power quality issues increases concerns within the research community [1]-[5]. Consequently, there is a need to develop different types of power quality conditioners to address these issues. Among the various power quality conditioners, active power filter topologies with different configurations have been used for solving the power quality problems. The growing demand for electricity in the recent age invites more and more renewable energy sources integration with the distribution network to fulfill the demand and maintain system stability [6]-[9]. However, the intermittent nature of renewable energy sources is a major concern when dealing with power quality and other issues [6]-[9]. Various

grid-connected photovoltaic (PV) system topologies have been presented and explored [6]-[12], accompanied by active filtering solutions aimed at preserving the quality of current in the supply system. While PV grid integration offers significant advantages over conventional systems, the presence of non-linear loads introducing voltage fluctuations in the system is also a major problem. So, it is important to design the filter with a proper controller in such a manner as to achieve enhanced power quality.

Traditionally, active power filters have relied on different controller includes synchronous reference theory, indirect current (ICC), sliding mode and unit vector template generation for generating reference signals which are treated as one of the most important parameters for the switching action of the filter [12]-[20]. While these techniques have been effective in generating reference signals and regulating voltage, achieving optimal performance often requires the integration of conventional proportional-integral (PI) controllers [16], [17]. However, PI controllers inherently possess limitations, notably non-zero steady-state errors, particularly in dynamic conditions. To address these limitations, researchers have turned to conventional optimization techniques [21]-[28]. These include genetic algorithms (GA), which mimic the process of natural selection to iteratively improve solutions, particle swarm optimization (PSO) [17], depends on the collective behavior of organisms like birds flocking or fish schooling, and differential evolution (DE), which optimize a problem by maintaining a population of candidate solutions and iteratively applying mutation, crossover, and selection operations. Despite their potential, these optimization techniques require careful tuning of parameters such as population size, mutation rates, and crossover probabilities, which can be challenging and computationally intensive. Additionally, each algorithm may have specific parameters, further complicating the optimization process. Furthermore, the convergence rate of these conventional optimization techniques can vary, leading to longer optimization times, and increased computational resources. Hence, while effective, conventional optimization techniques may not always provide optimal solutions within acceptable timeframes.

Real-world constraints, such as hardware limitations, cost considerations, and environmental factors, further complicate the optimization process, necessitating the consideration of trade-offs between computational complexity and solution quality. Moreover, the advent of multi-objective optimization highlights the need to balance conflicting objectives, such as minimizing both cost, and energy consumption. Researchers are exploring adaptive optimization techniques that can dynamically adjust their parameters or algorithms based on changing conditions, as well as hybrid optimization approaches that combine multiple techniques to leverage their respective strengths and mitigate their weaknesses. Additionally, addressing uncertainty in optimization problems, such as uncertain system parameters or environmental disturbances, remains a significant challenge, with robust optimization techniques offering potential solutions. Despite these challenges, ongoing research aims to enhance optimization strategies, ultimately improving the performance of active power filter systems. Jaya optimization algorithm [6], [7], [14] possess an improved solution as it depends on the various controlling parameter, but this dependability increases the number of iterations to obtained the best and worst cases from the whole solution. To overcome the issue, an enhanced Jaya optimization scheme is proposed by the authors, in this scheme, first population from best to worst is sorted and two groups are formed as "Best" and "Worst", "Best" is the best solution from the best solution group and similarly "Worst" is the result of best solution from the worst solution group, this modification decreases the number of iteration to obtained the optimal solution.

From the introduction, it is noticed that the implementation of the Jaya optimization algorithm has been carried out in many problems, including electrical engineering, as well as for improving the performance of different types of controllers. Particularly in power quality problems, it has also been implemented in many papers. We have modified Jaya and implemented it in a PV-SAPF. Although Jaya implementation has been done in many works, the performance of modified Jaya along with indirect current control technique has not been investigated so far. We have implemented it in this work.

The new finding is the development of the modified Jaya algorithm along with the indirect current control technique and its implementation in the controller part of the proposed PV-SAPF to improve the filtering capacity of harmonics which develops due to the nonlinearity nature of load and results in better quality of power. The entire contribution of the work is listed: i) Modification of the existing Jaya, its implementation with PI and ICC to generate the reference signal; ii) Development of the PV-SAPF; iii) Proper implementation of all the developed controller in PV-SAPF; and iv) Performance evaluation with various loads as case study to the distribution system. The structure of the paper are: i) Section 1 introduction and it includes the literature review, problem formulation, and main contributions by the authors; ii) A detailed description of the proposed methodology, including the PV-based series filter, is presented in section 2; iii) The methods possess the controller is discussed in section 3; iv) Section 4, complete description of the simulation results and its analysis is presented; and v) Last, section 5 overall conclusions of the work is presented.

2. PROPOSED METODOLOGY

Power quality improvement using different methodologies in the distribution sector is discussed in the introduction section. Different types of work in this area with the development of various power conditioners equipment has been studied and performance also investigated, for better results more findings are required and still scope is there to design and develop new device to enhance the power quality performance. Keeping this in mind, a PV-SAPF is developed and its performance is analyzed with different methods involving control techniques to control and regulate various parameters.

The schematic PV-SAPF with the system shown in Figure 1. PV array, utility grid loads are connected through the SAPF, the output of the SAPF is fed to the point of common coupling, SAPF consists of a three-phase voltage source converter which acts as the filters and a converter transformer. Load consists of rectifier along with resistive-inductive, resistive-capacitive and resistive-inductive-capacitive are connected to system to investigate the performance. Voltage related problem is intentionally developed in the system and injecting voltage signal of the filter is analyzed, source resistance and inductance values are represented as R_s, L_s respectively, resistances and inductances connected in-between inverter to grid represented as R_f, L_f , the direct current (DC) link capacitor is represented as the parameters in the designed problem are mentioned in Table 1.

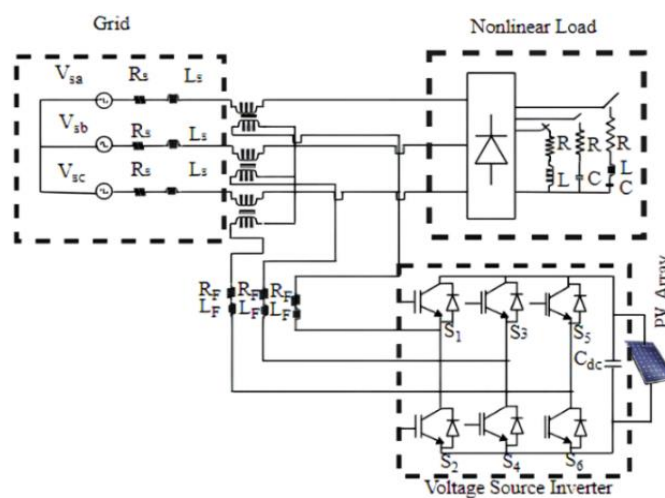


Figure 1. Propose PV fed series active power filter

Table 1. Parameters and its values

Sl.no	Parameter	Values
1	Grid capacity voltage	600 Volt
2	Frequency	50 Hz
3	DC bus capacitor	3000 μ F
4	Grid side inductance	2.5 mH
5	Inverter side inductance	3 mH
6	Load resistance, inductance, and capacitance	300 Ω , 0.2 mH, 55 μ F

3. PROPOSED METHOD-CONTROLLER IN PV-SAPF

PV-SAPF performance mainly depends on the controller and how the implementation of the controller is carried out, effective implementation is able to develop the accurate generation of the signal and proper tuning of various parameters which are the most important requirements apart from other necessary conditions. Modified Jaya with PI, indirect current control techniques or ICCT are used to generate the reference signal and compared with the actual signal, error signal fed to hysteresis controller to obtain the pulses of the PV-SAPF. The details procedure to obtain the error signal with the proposed controller is described in details in the below steps along with the mathematical analysis.

3.1. Indirect current control techniques (ICCT)

Indirect current controller techniques [16] is used along with other described above techniques to developed the accurate reference source current, in this technique, real component is extracted from the fundamental component. The mathematical equations are formulated by taking the load signal which constitute fundamental and harmonics in each phase from (1)-(3).

$$i_{La} = I_{La1} \sin(\omega t - \varphi_{a1}) + \sum_{n=2}^{\infty} I_{Lan} \sin(n\omega t - \varphi_{an}) \quad (1)$$

$$i_{Lb} = I_{Lb1} \sin(\omega t - \varphi_{b1}) + \sum_{n=2}^{\infty} I_{Lbn} \sin(n\omega t - \varphi_{bn}) \quad (2)$$

$$i_{Lc} = I_{Lc1} \sin(\omega t - \varphi_{c1}) + \sum_{n=2}^{\infty} I_{Lcn} \sin(n\omega t - \varphi_{cn}) \quad (3)$$

Obtained real component are as (4)-(6).

$$I_{sam} = |I_{La1}| \cos \varphi_1 \quad (4)$$

$$I_{sbm} = |I_{Lb1}| \cos \varphi_1 \quad (5)$$

$$I_{scm} = |I_{Lc1}| \cos \varphi_1 \quad (6)$$

When the system is on operation the switching action of the filter results reduction of DC link voltage due to some amount of internal power loss and also deviation of voltage can be noticed due to same losses in the filter and instant variation of the load. To maintain the stability of the system and other proper work, it is essential and necessary to maintain constant voltage at DC link during the operation of the system. The DC link voltage at every instant is continuously monitored with the help of sensors and compared to the reference, the error generates is fed to PI and finally the output from PI is added with the amplitude of the source current and utilize for compensations. Peak current for a balanced system is represented in (7).

$$I_{sm} = \left(\frac{I_{sam} + I_{sbm} + I_{scm}}{3} \right) + I_{sL} \quad (7)$$

To obtain ideal compensation, it is better to consider the reference signal as pure signal of magnitude I_{sm} and in phase with the grid voltage, multiplication of the calculated peak magnitude and unit template results the required reference, it is represented in (8)-(10).

$$i_{sa}^* = I_{sm} U_a = I_{sm} \sin(\omega t) \quad (8)$$

$$i_{sb}^* = I_{sm} U_b = I_{sm} \sin(\omega t - 120^\circ) \quad (9)$$

$$i_{sc}^* = I_{sm} U_c = I_{sm} \sin(\omega t + 120^\circ) \quad (10)$$

Once the generation of the reference source current is over, for more accuracy reference filter signal is generated and it is compared with the actual filter current, based on the requirement the switching action is carried out using the hysteresis current controller.

3.2. Enhanced JAYA optimization technique

Jaya algorithm used in various area as it has possess large solution space to reach the optimal solution in a define problem, the capability of solving both constrained and unconstrained optimization problems with Jaya is effectively investigated [6], [7], [14], repeatedly modification of population of individual solution is one of the important criteria in this algorithm and it is also consider as a gradient-free algorithm for optimization problem, the variables of the lower bound L_b and upper bound U_b are considered as the objective function, setting of the termination criteria after defining search space is one of the required condition satisfies stopping execution of the algorithm. The next step is the initialization of the population or the develop of random solutions within specified range of variables in a define problem, for accuracy, updating population at every iteration using different strategy is important aspect in the algorithm. it is usually noticed the algorithm always try to keep good solution and try to out inferior solution. Traditional algorithms use both algorithm specific control parameter and control parameters like inertia weight in case of PSO, number of onlooker and employed bees in case of ant colony bee algorithm. but Jaya excluded from algorithm specific but more focus is on control parameters like population size. it is economical and it also gives suitable platform for discrete optimization. Another important characteristic is the fast response Here we are using Jaya optimization algorithm to determine suitable values for proportional gain k_p and Integral gain k_i for PI controller.

The detailed steps of modified. Jaya implementation in the proposed system are presented as:

- Step 1: Formulation of the objective function $f(x)$, initialization of population size, design variables, limits of upper and lower design variables and the termination criterion. Parameter representation: $p = 1, 2, 3, \dots, n$, $d = 1, 2, 3, \dots, m$, U_L, L_L , $k = i = 1, 2, 3, \dots, K$
- Step 2: Generation of random population, taking the population size and design variables in to consideration

- Step 3: Identification of best and worst solutions in the population
- Step 4: Modification of the solution based on the best and worst solutions
- Step 5: Comparative analysis of the present value with the previous iteration value, updating is carried out at the end of i^{th} iteration based on fitness
- Step 6: Repeat steps 3, 4, and 5 until the termination criteria is reached

As it is discussed, in modified Jaya, an enhanced Jaya optimization scheme is proposed by the authors, in this scheme, first population from best to worst is sorted and two groups are formed as "Best" and "Worst", "Best" is the best solution from the best solution group and similarly "Worst" is the result of best solution from the worst solution group, this modification decreases the number of iteration to obtain the optimal solution.

The mean square error (MSE) in [5] is used in this paper as the objective function ' J ' for the specific optimization problem, as in (11). The error signal is presented in (12). Figure 2(a) is shown Jaya algorithm and modified Jaya is presented in Figure 2(b).

$$J = \text{MSE} = \sum_{i=1}^{\text{ITER}} e_r^2 \quad (11)$$

$$\frac{|i_{f2a}^* - i_{f2a}| + |i_{f2b}^* - i_{f2b}| + |i_{f2c}^* - i_{f2c}| + |V_{\text{RefPV}} - V_{\text{PV}}|}{\text{ITER}} \quad (12)$$

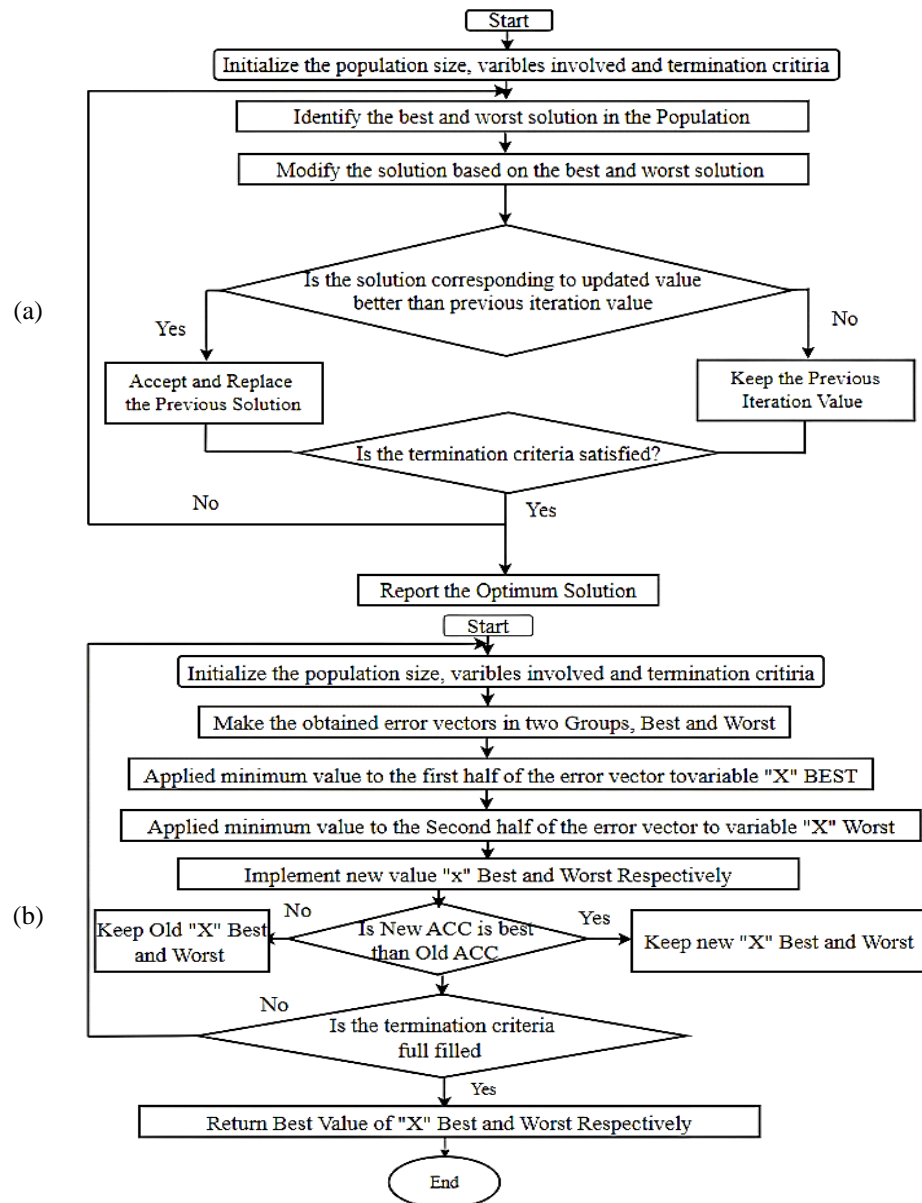


Figure 2. Flowchart of optimization: (a) Jaya algorithm and (b) modified Jaya algorithm

3.3. Hysteresis current control (HCC) technique

To achieve proper and better switching action of the inverters, HCC [9], [18] is employed in this work. The error obtained from reference filter current and actual filter current signal is fed to the HCC, as the switching frequency is not constant throughout the power frequency cycle; it keeps changing in time with the operating point. Regulation of the switching pattern of the active filter for the required output is accomplished by the hysteresis band. This control technique is chosen for switching action due to its advantages of quick controllability and simple implementation. The complete controller block diagram is presented in Figure 3(a), along with the HCC in Figure 3(b).

To ensure proper and accurate operation of the series active filter, the above-mentioned controllers work jointly as described in their respective sections. Figure 3(a) shows the block diagram of the controller which provides an idea: after tuning and optimizing PI controller gains, it generates a current signal combining the fundamental real component to produce maximum source current. This signal is further combined with the output of the unit vector (UV) template generation to yield the reference source signal, which is then used to generate the reference filter current. The advantages of the enhanced Jaya-optimized PV-fed series active filter include requiring a lower rating of voltage source inverter, which can operate with DC link voltage of low value. Additionally, it exhibits a faster convergence rate to achieve global optimum. Furthermore, this method improves the current compensating capacity in various disturbances that often arise in a distribution system.

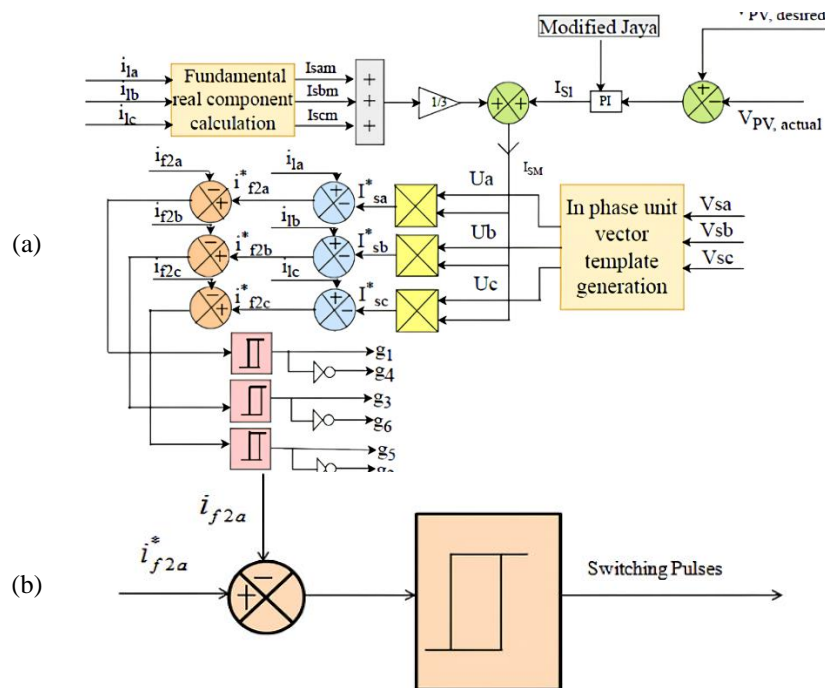


Figure 3. Proposed controller: (a) controller block diagram and (b) hysteresis current controller

4. RESULT AND DISCUSSION

The fruitfulness of controller with the proposed system is verified by connecting various types of loads to the system. Rectifiers with load R-L, load R-C, and load R-L-C configurations are connected. The total-harmonic-distortion (THD) is recorded both without and with optimization [14]. The various parameters of the algorithm modified. Jaya are taken from, and a comparative analysis without and with modified optimization techniques is presented. In each case, THD analysis is conducted and presented.

4.1. PV-series active power (PV-SAF) filter without optimization–rectifier with load R-L

In this case, input source is connected to resistive and inductive (R-L) load and the output of the PV-SAF is verified. After compensation the DC link voltage, load voltage, injected voltage, and grid voltage are presented in Figures 4(a)–4(d). THD analysis of grid voltage after compensation is presented in Figure 5. From its analysis, it is found that after filtration still harmonics components are present which 7.04% of the fundamental component is. After compensation, the FFT analysis of grid voltage is presented in Figure 5. It is observed after filtration, still harmonics components are present which 7.04% of the fundamental component, THD in each of the harmonics present in Table 2.

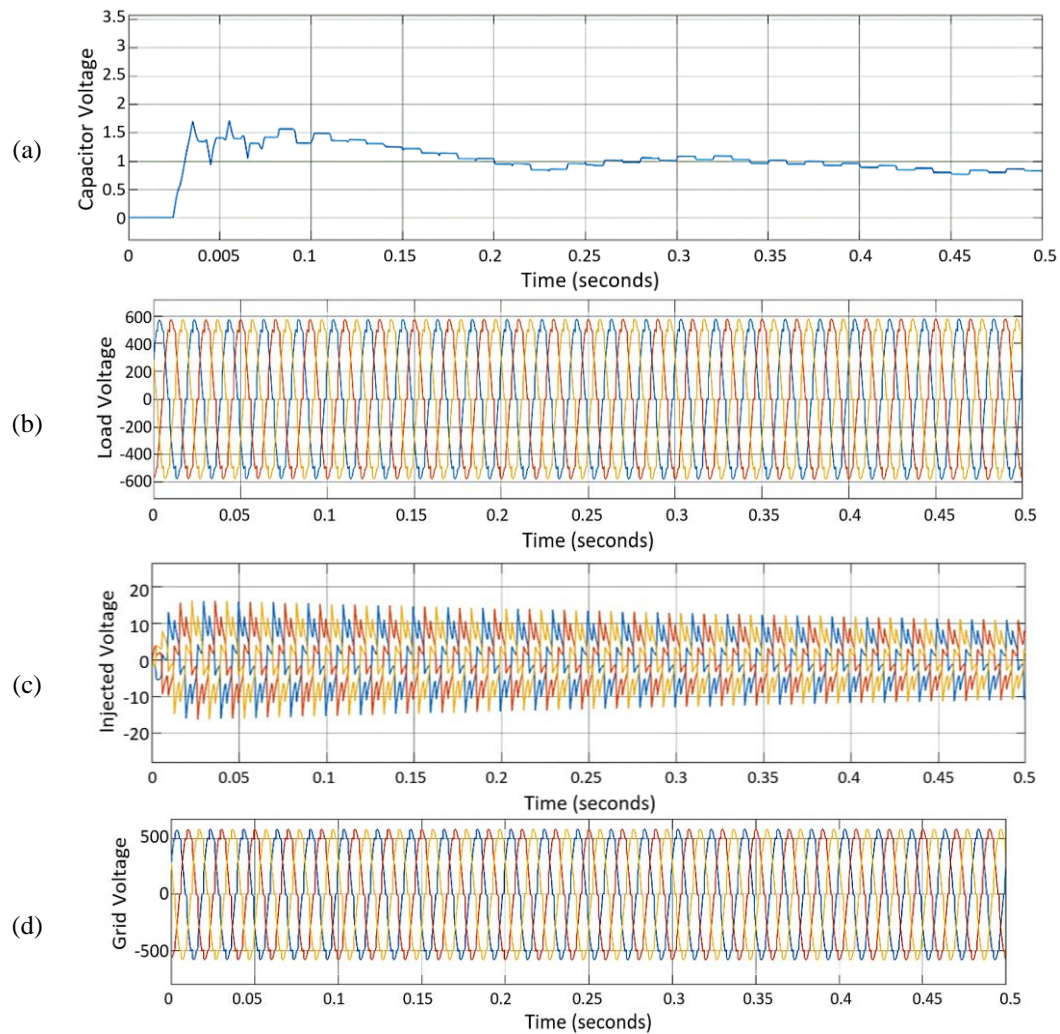


Figure 4. PV-SAPF without optimization–rectifier with load R-L: (a) capacitor voltage, (b) load voltage, (c) injected voltage, and (d) grid voltage after filtration

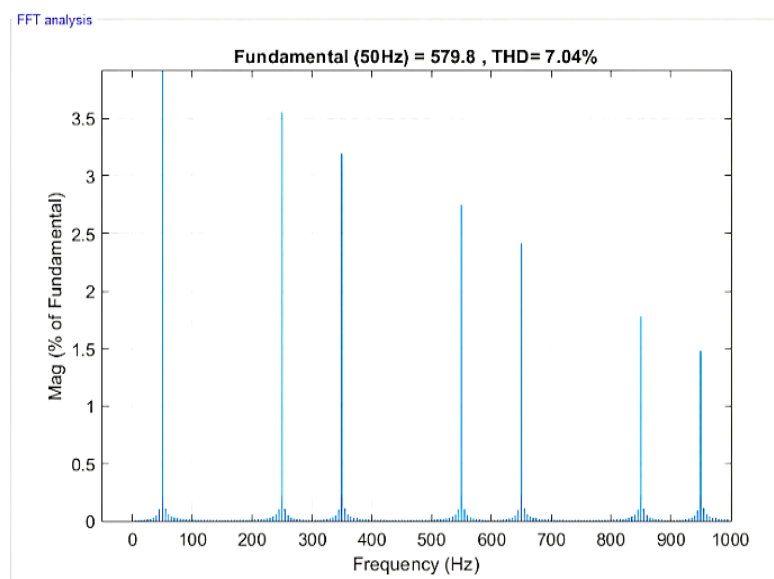


Figure 5. THD after filter without optimization

Table 2. THD in each harmonic's parameter

Sl.no	Frequency in HZ	THD in percentage	Sl.no	Frequency in HZ	THD in percentage
1	50	100	4	350	3.20
2	150	0.01	5	450	0.01
3	250	3.55	6	550	2.75

4.2. PV-series active power filter (PV-SAPF) with optimization–rectifier with load R-L

In this case, the same system is followed but optimization technique applied to PI controller to optimize the gains which significantly improves the output of the capacitor voltage. This improvement of the capacitor voltage increases the performance of the PV-SAPF results the reduction of THD level to 4.67% of the fundamental. The analysis is acceptable by IEEE 519.4. After compensation, wave form of DC link voltage, load voltage, injected voltage and grid voltage are shown from Figures 6(a)-6(d) respectively. After compensation, the FFT analysis of grid voltage is presented in Figure 7. It is observed after filtration, the achieved THD level is coming under IEE519 and it is quite satisfactory. Due to enhanced Jaya optimization the compensation level increases, THD in each of the harmonics present in Table 3.

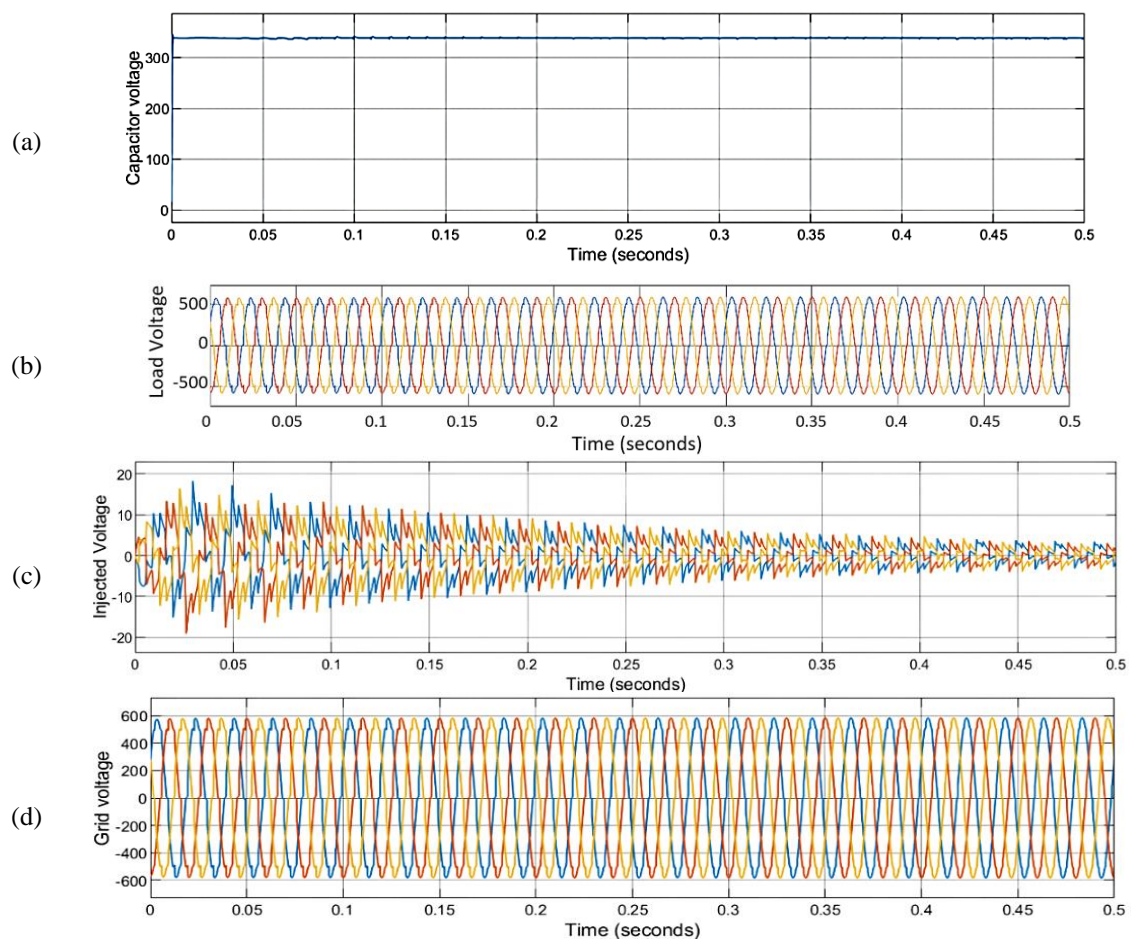


Figure 6. PV-SAPF with optimization–rectifier with load R-L: (a) capacitor voltage, (b) load voltage, (c) injected filter voltage, and (d) grid voltage after filtration

Table 3. THD in each harmonic's parameter

Sl.no	Frequency in HZ	THD in percentage	Sl.no	Frequency in HZ	THD in percentage
1	50	100	4	350	1.81
2	150	0.02	5	450	0.02
3	250	2.02	6	550	1.70

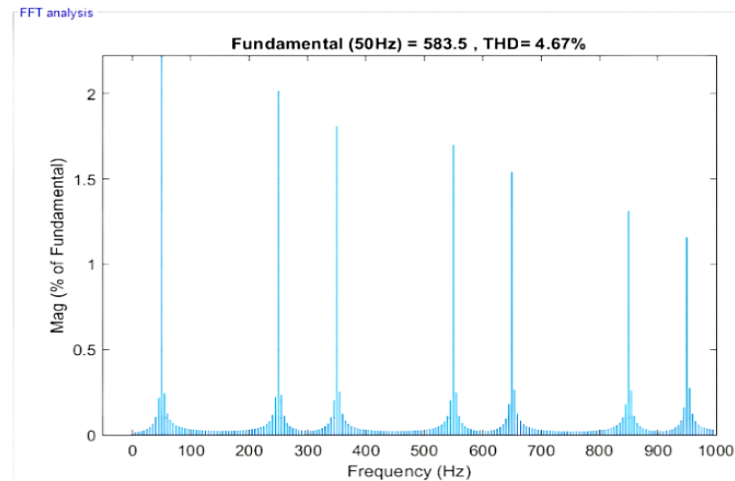


Figure 7. THD after filter without optimization

4.3. PV-SAF filter without optimization–rectifier with load R-C

In this case the supply is fed to a load R-C and the performance of the PV-SAF filter is verified, connecting the PV in the system. After compensation the wave form of the DC link voltage, load voltage, injected voltage, and grid voltage are shown from Figures 8(a)-8(d), THD analysis of source current after compensation is presented in Figure 9, and it is 8.31% of the fundamental which is not very much effective. From that figure, it is slightly improved. After compensation, fast Fourier transform analysis of grid voltage is shown in Figure 9, from analysis; it is found that after filtration still harmonics components are present which 8.31% of the fundamental component, THD in each of the harmonics present in Table 4.

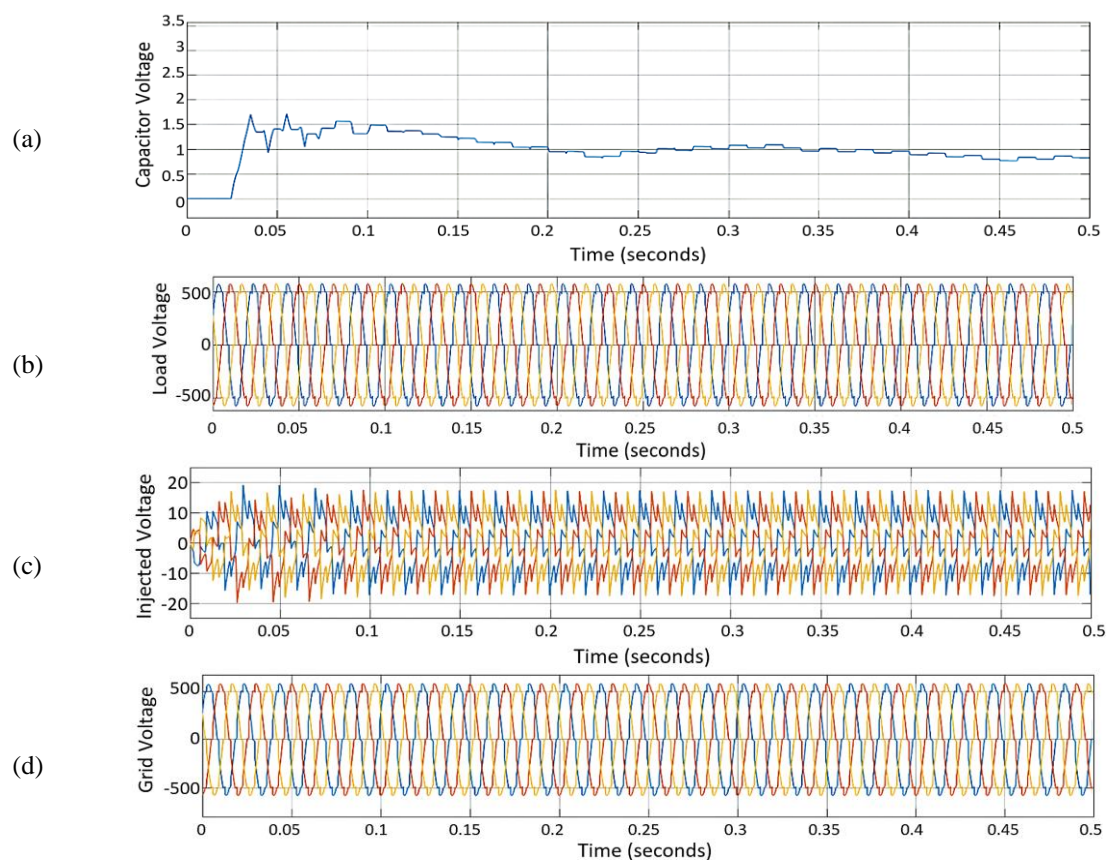


Figure 8. PV-SAPF without optimization –rectifier with load R-C: (a) capacitor voltage, (b) load voltage, (c) injected voltage, and (d) grid voltage after filtration

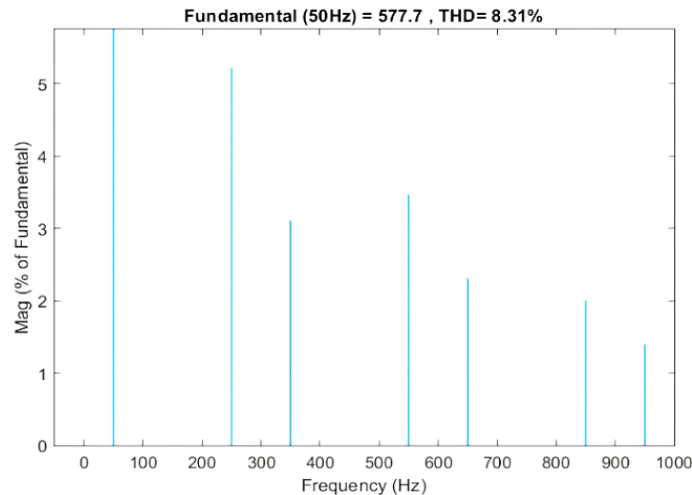


Figure 9. THD after filter without optimization

Table 4. THD in each harmonic's parameter

Sl.no	Frequency in HZ	THD in percentage	Sl.no	Frequency in HZ	THD in percentage
1	50	100	4	350	3.12
2	150	3.03	5	450	0.00
3	250	5.23	6	550	3.47

4.4. PV-SAPF filter with optimization–rectifier with load R-C

In this case, the same system is followed but optimization technique applied to PI controller to optimize the gains which significantly improves the output of the capacitor voltage. This improvement of the capacitor voltage increases the performance of the PV-SAPF results the reduction of THD level to 4.51% of the fundamental. The result is acceptable by IEEE 519. 4. After compensation, the output of DC link voltage, load voltage, injected voltage and grid voltage is presented in Figures 10(a)-10(d) respectively. After compensation, THD analysis of grid voltage is presented in Figure 11. After compensation, the FFT analysis of grid voltage after compensation is shown in Figure 11. From analysis, it is found that after filtration still harmonics components are present which 4.51% of the fundamental component, THD in each of the harmonics present in Table 5.

4.5. PV-SAF filter without optimization–rectifier with load R-L-C

Here, supply is fed to load R-L-C and the PV-SAF filter performance is verified. After compensation, the DC link voltage, load voltage, injected voltage, and grid voltage are presented in Figures 12(a)-(d). After compensation, fast Fourier transform analysis of supply current is presented in Figure 13. THD is 7.16% of the fundamental which cannot be acceptable. After compensation, the FFT analysis of grid voltage show in Figure 13, and from this analysis; it is found that after filtration still harmonics components are present which 7.16% of the fundamental component, THD in each of the harmonics present in Table 6.

4.6. PV-SAPF filter with optimization–rectifier with load R-L-C

In this case, the same system is followed but optimization technique applied to PI controller to optimize the gains which significantly improves the output of the capacitor voltage. This improvement of the capacitor voltage increases the performance of the PV-SAPF results in the reduction of THD level to 4.72% of the fundamental value. Now, this is acceptable by IEEE 519. 4. After compensation, voltage of DC link, load voltage, injected voltage, and grid voltage are shown in Figures 14(a)-14(d) respectively. After compensation, the FFT analysis of grid voltage is presented in Figure 15.

After compensation, the FFT analysis of grid voltage is presented in Figure 15. from analysis; it is found that after filtration 4.72% of the fundamental component is achieved which is comes under IEEE 519 THD in each of the harmonics present in Table 7. The FFT analysis in all types of load connected to the system is shown in a tabular form for quick analysis in Table 8. The chart diagram of the THD analysis followed by Table 8 without and with optimization techniques with various loads is presented in Figure 16.

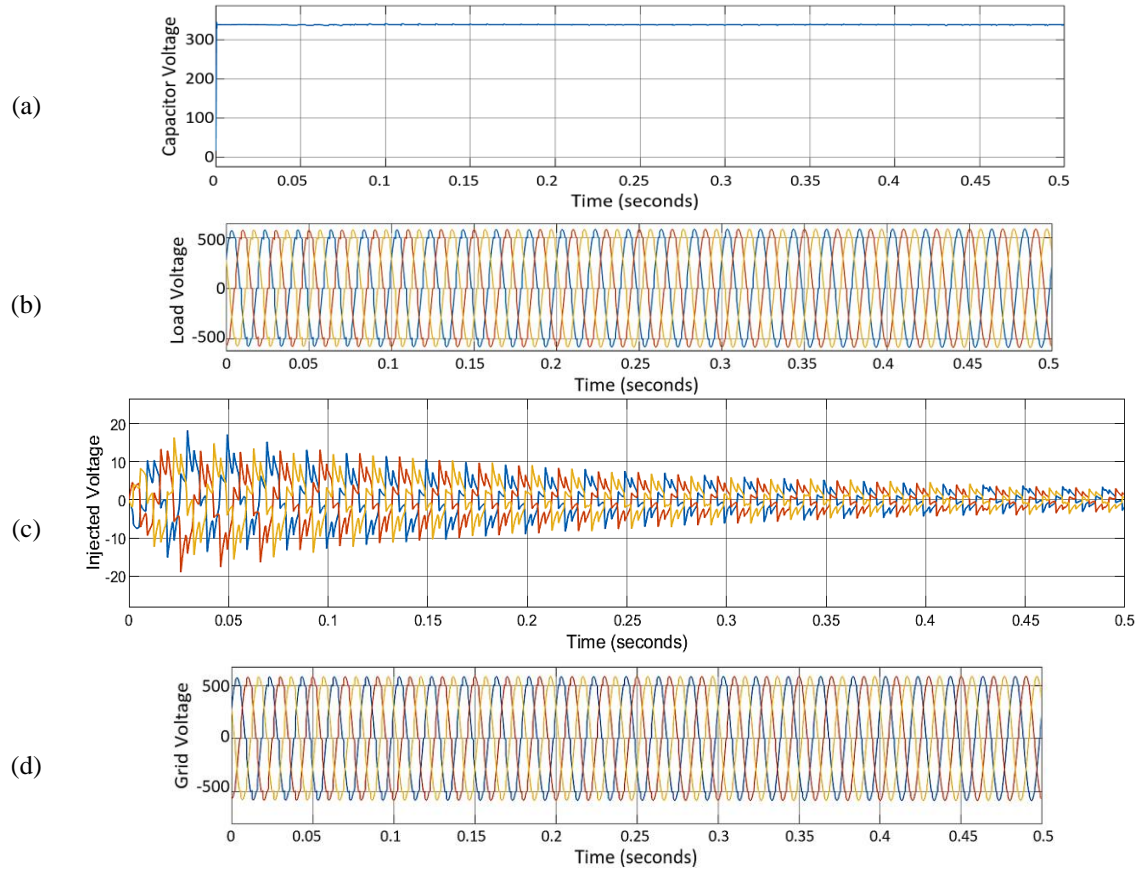


Figure 10. PV-SAPF with optimization-rectifier with load R-C: (a) capacitor voltage, (b) load voltage, (c) injected voltage, and (d) grid voltage after filtration

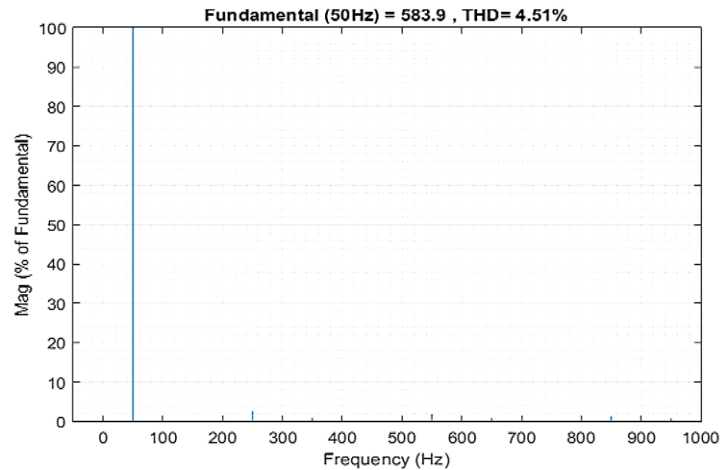


Figure 11. THD after filter without optimization

Table 5. THD in each harmonic's parameter

Sl.no	Frequency in HZ	THD in percentage
1	50	100
2	150	0.33
3	250	2.72
4	350	1.96
5	450	0.07
6	550	1.90

Table 6. THD in each harmonic's parameter

Sl.no	Frequency in HZ	THD in percentage
1	50	100
2	150	2.13
3	250	3.27
4	350	3.93
5	450	1.36
6	550	3.47

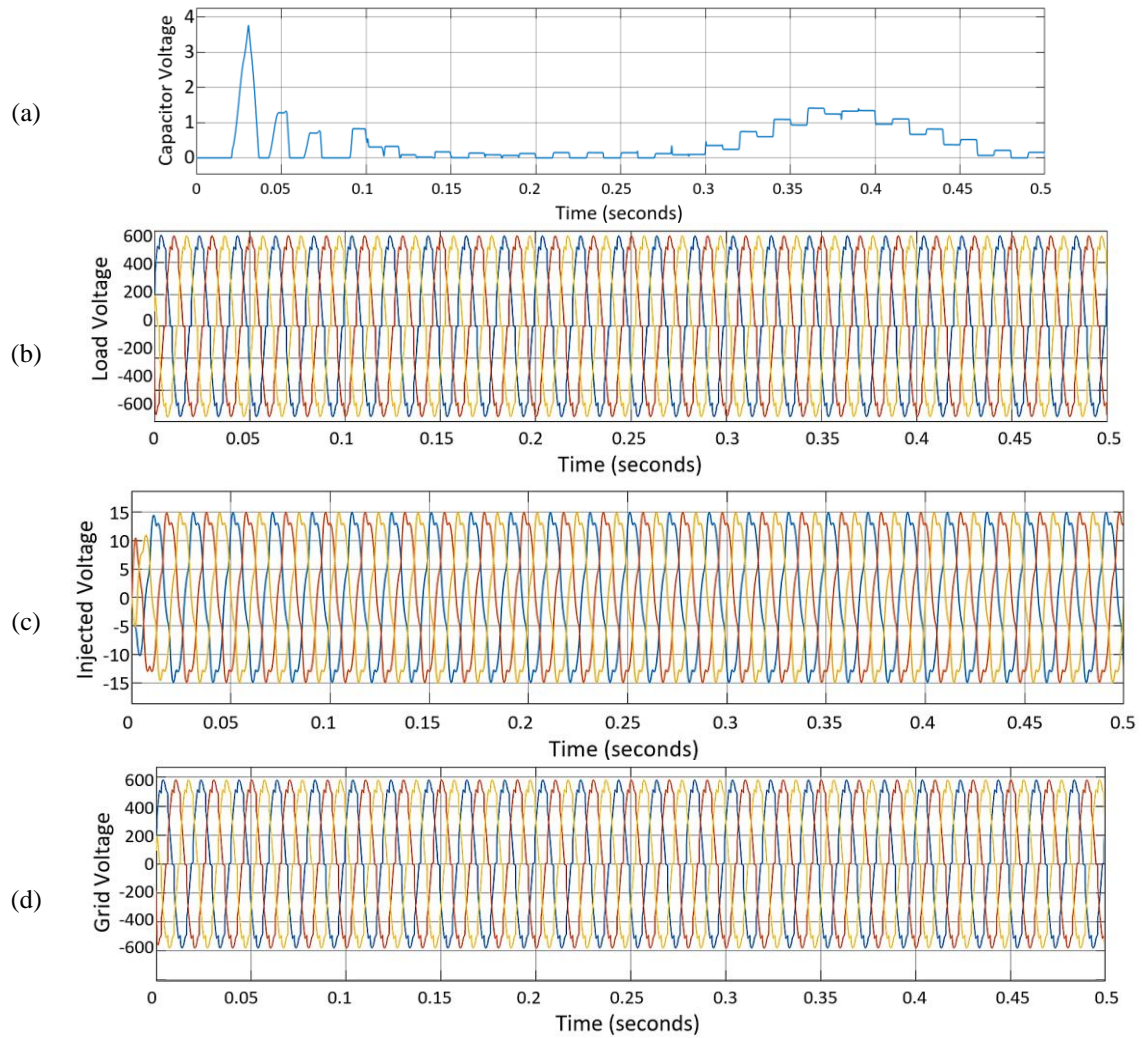


Figure 12. PV-SAPF without optimization–rectifier with load R-L-C:(a) capacitor voltage, (b) load voltage, (c) injected voltage, and (d) grid voltage after filtration

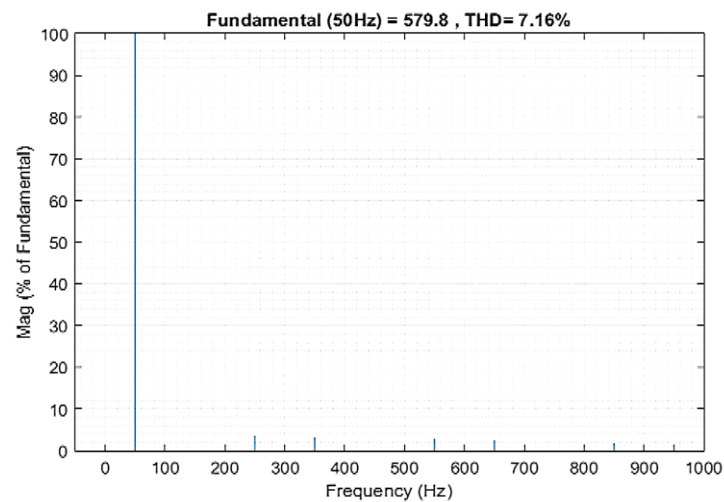


Figure 13. THD after filter without optimization

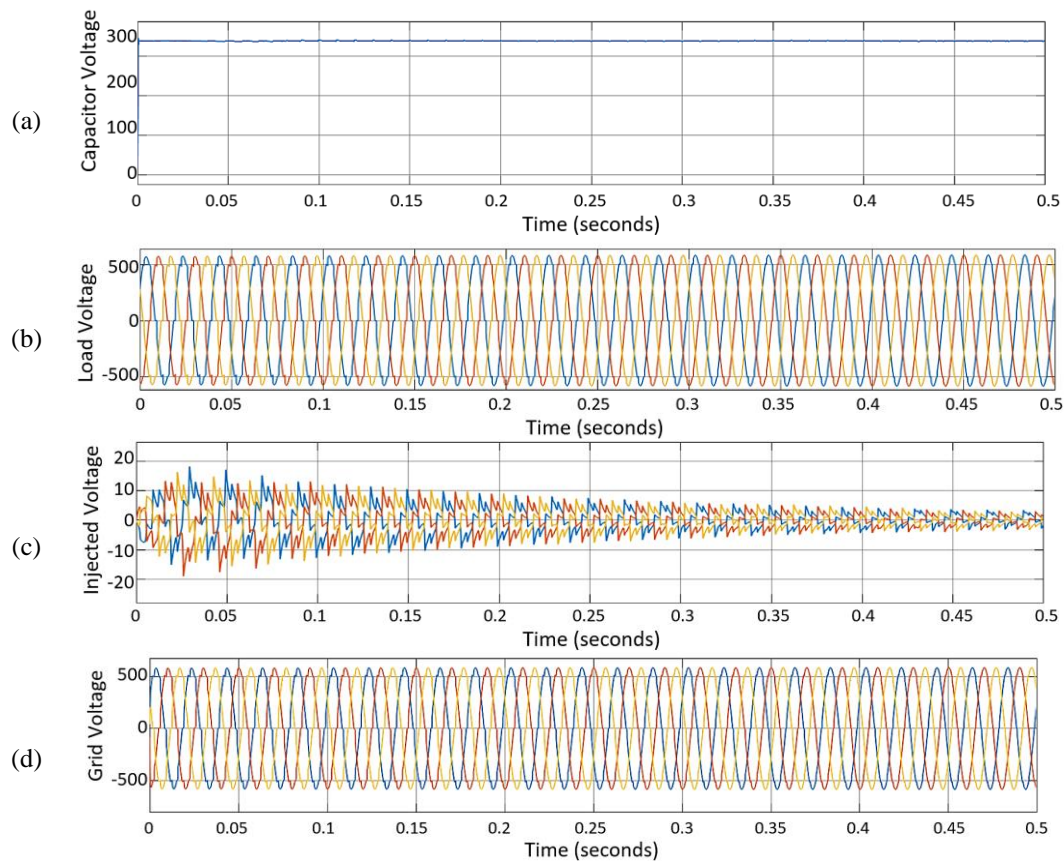


Figure 14. PV-SAPF with optimization –rectifier with load R-L-C load (a) capacitor voltage, (b) load voltage, (c) injected voltage, and (d) grid voltage after filtration

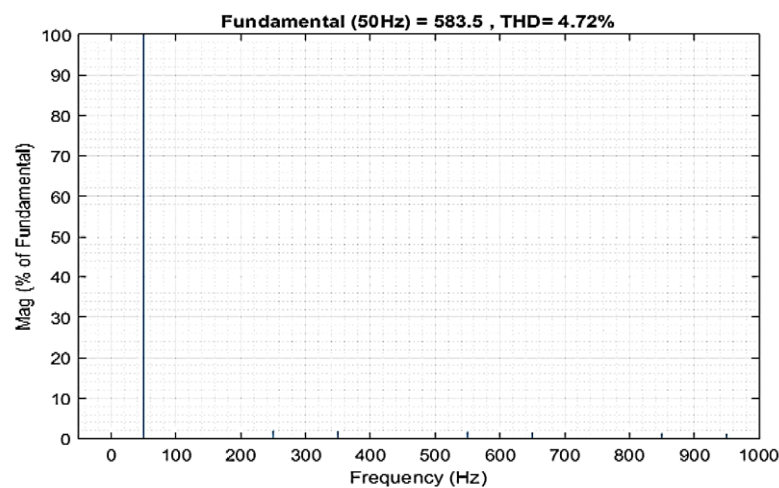


Figure 15. THD after filter without optimization

Table 7. THD in each harmonic's parameter

Sl.no	Frequency in HZ	THD in percentage
1	50	100
2	150	1.13
3	250	2.27
4	350	1.93
5	450	1.26
6	550	2.47

Table 8. THD Analysis in each case without and with optimization

R-L without optimization	R-L with optimization	THD in percentage with fundamental		R-L-C without optimization	R-L-C with optimization
		R-C without optimization	R-C with optimization		
7.04	4.67	8.31	4.51	7.16	4.72

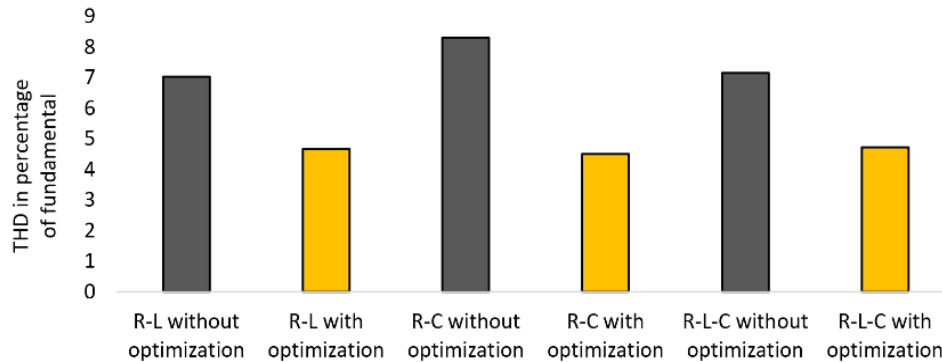


Figure 16. Chat diagram of THD analysis without and with optimization technique

5. CONCLUSIONS

In this research work, the developed controller combines both modified Jaya and indirect current control techniques is successfully implemented in PV-SAPF filter for improving filtering capacity that leads to distribution system power quality improvement. Fruitfulness of the suggested active power filter is verified with various loads, with and without optimization techniques. From the table of total harmonic distortion analysis, it is found that in each case, indirect current control techniques along without optimized Jaya, the THD is more than 5% of the fundamental which is not acceptable by IEEE 519. However, when optimized modified Jaya along with indirect current control implemented the THD value comes under acceptable level of IEEE 519 which is below 5% of the fundamental in all the cases. Not only with lowering the THD value the suggested optimized controller, but also it is able to improve the reactive power apart from maintain stable capacitor voltage.




REFERENCES

- [1] H. Akagi, "New trends in active filters for power conditioning," *IEEE Transactions on Industry Applications*, vol. 32, no. 6, pp. 1312–1322, 1996, doi: 10.1109/28.556633.
- [2] B. Singh, C. Jain, S. Goel, R. Gogia, and U. Subramaniam, "A sustainable solar photovoltaic energy system interfaced with grid-tied voltage source converter for power quality improvement," *Electric Power Components and Systems*, vol. 45, no. 2, pp. 171–183, Jan. 2017, doi: 10.1080/15325008.2016.1233298.
- [3] B. Singh, A. Chandra, and K. Al-Haddad, *Power quality problems and mitigation techniques*. Wiley, 2015. doi: 10.1002/9781118922064.
- [4] B. K. Santhoshi, K. M. Sundaram, S. Padmanaban, J. B. Holm-Nielsen, and P. K. K., "Critical review of PV grid-tied inverters," *Energies*, vol. 12, no. 10, p. 1921, May 2019, doi: 10.3390/en12101921.
- [5] H. K. Al-Hadidi, A. M. Gole, and D. A. Jacobson, "A novel configuration for a cascade inverter-based dynamic voltage restorer with reduced energy storage requirements," *IEEE Transactions on Power Delivery*, vol. 23, no. 2, pp. 881–888, Apr. 2008, doi: 10.1109/TPWRD.2007.915989.
- [6] S. K. Dash and P. K. Ray, "Power quality improvement utilizing PV fed unified power quality conditioner based on UV-PI and PR-R controller," *CPSS Transactions on Power Electronics and Applications*, vol. 3, no. 3, pp. 243–253, Sep. 2018, doi: 10.24295/CPSPTEA.2018.00024.
- [7] S. Mishra and P. K. Ray, "Power quality improvement using photovoltaic fed DSTATCOM based on JAYA optimization," *IEEE Transactions on Sustainable Energy*, vol. 7, no. 4, pp. 1672–1680, Oct. 2016, doi: 10.1109/TSTE.2016.2570256.
- [8] N. D. Tuyen and G. Fujita, "PV-active power filter combination supplies power to nonlinear load and compensates utility current," *IEEE Power and Energy Technology Systems Journal*, vol. 2, no. 1, pp. 32–42, Mar. 2015, doi: 10.1109/JPETS.2015.2404355.
- [9] E. Madhurima, P. S. Puhana, and S. K., "Performance analysis of photovoltaic fed series active power filter for power quality improvement," in *2020 3rd International Conference on Energy, Power and Environment: Towards Clean Energy Technologies*, IEEE, Mar. 2021, pp. 1–6. doi: 10.1109/ICEPE50861.2021.9404501.
- [10] M. Antchev, V. Gourgoulitsov, and H. Antchev, "Study of the operation of the output filter of a single-phase series active power filter," *International Journal of Power Electronics and Drive Systems (IJPEDS)*, vol. 12, no. 1, pp. 304–313, Mar. 2021, doi: 10.11591/ijpeds.v12.i1.pp304-313.
- [11] S. N. Setty, M. S. D. Shashikala, and K. T. Veeramanju, "Hybrid control mechanism-based DVR for mitigation of voltage sag and swell in solar PV-based IEEE 33 bus system," *International Journal of Power Electronics and Drive Systems (IJPEDS)*, vol. 14, no. 1, pp. 209–221, Mar. 2023, doi: 10.11591/ijpeds.v14.i1.pp209-221.




- [12] T. K. Benamar, A. Allali, H. M. Boulouiha, and M. Denai, "Voltage profile and power quality improvement using multicell dynamic voltage restorer," *International Journal of Power Electronics and Drive Systems (IJPEDS)*, vol. 13, no. 4, pp. 2216–2225, Dec. 2022, doi: 10.11591/ijpeds.v13.i4.pp2216-2225.
- [13] E. R. Ribeiro and I. Barbi, "Harmonic voltage reduction using a series active filter under different load conditions," *IEEE Transactions on Power Electronics*, vol. 21, no. 5, pp. 1394–1402, Sep. 2006, doi: 10.1109/TPEL.2006.880265.
- [14] K. P. Vineeth, P. S. Puhana, S. Sahoo, and K. S. Reddy, "Performance comparison of different controller implementation in a PV fed SAPF," in *Sustainable Energy and Technological Advancements. ISSETA 2023*, 2023, pp. 225–238. doi: 10.1007/978-981-99-4175-9_19.
- [15] P. S. Puhana, P. K. Ray, and G. Panda, "A comparative analysis of shunt active power filter and hybrid active power filter with different control techniques applied for harmonic elimination in a single phase system," *International Journal of Modelling, Identification and Control*, vol. 24, no. 1, pp. 19–28, 2015, doi: 10.1504/IJMIC.2015.071698.
- [16] G. Pingping, L. Ziguang, L. Zhuo, and W. Di, "PI-PSO algorithm based voltage controller of STATCOM for self-excited induction generator," in *2015 34th Chinese Control Conference (CCC)*, IEEE, Jul. 2015, pp. 4349–4354. doi: 10.1109/ChiCC.2015.7260313.
- [17] R. Mallajoshula and I. E. S. Naidu, "Novel MAF-fuzzy based IR-SRF controller for DVR to improve PQ under dynamic weak grid conditions," *IETE Journal of Research*, vol. 69, no. 10, pp. 7515–7540, Oct. 2023, doi: 10.1080/03772063.2021.2021821.
- [18] M. Castilla, J. Miret, A. Camacho, J. Matas, and L. G. de Vicuna, "Voltage support control strategies for static synchronous compensators under unbalanced voltage sags," *IEEE Transactions on Industrial Electronics*, vol. 61, no. 2, pp. 808–820, Feb. 2014, doi: 10.1109/TIE.2013.2257141.
- [19] C. Lascu, L. Asiminoaei, I. Boldea, and F. Blaabjerg, "High performance current controller for selective harmonic compensation in active power filters," *IEEE Transactions on Power Electronics*, vol. 22, no. 5, pp. 1826–1835, Sep. 2007, doi: 10.1109/TPEL.2007.904060.
- [20] P. S. Puhana, P. K. Ray, and S. Pottapinjara, "Performance analysis of shunt active filter for harmonic compensation under various non-linear loads" *International Journal of Emerging Electric Power Systems*, vol. 22, no. 1, pp. 21–29, 24 Feb. 2021, doi: 10.1515/ijeeps-2020-0197.
- [21] G. Panda, P. K. Ray, P. S. Puhana, and S. K. Dash, "Novel schemes used for estimation of power system harmonics and their elimination in a three-phase distribution system," *International Journal of Electrical Power & Energy Systems*, vol. 53, pp. 842–856, Dec. 2013, doi: 10.1016/j.ijepes.2013.05.037.
- [22] S. D. Swain, P. K. Ray, and K. B. Mohanty, "Voltage compensation and stability analysis of hybrid series active filter for harmonic components," in *2013 Annual IEEE India Conference (INDICON)*, IEEE, Dec. 2013, pp. 1–6. doi: 10.1109/INDICON.2013.6726005.
- [23] A. Bag, B. Subudhi, and P. K. Ray, "Grid integration of PV system with active power filtering," in *2016 2nd International Conference on Control, Instrumentation, Energy & Communication (CIEC)*, IEEE, Jan. 2016, pp. 372–376. doi: 10.1109/CIEC.2016.7513810.
- [24] M. P. Behera, P. K. Ray, and G. H. Beng, "Single-phase grid-tied photovoltaic inverter to control active and reactive power with battery energy storage device," in *2016 IEEE Region 10 Conference (TENCON)*, IEEE, Nov. 2016, pp. 1900–1904. doi: 10.1109/TENCON.2016.7848352.
- [25] P. S. Puhana, A. Valla, and S. Sahoo, "Performance investigation of L-type shunt active power filter supported with battery using UVT control method for distorted loads," in *2020 3rd International Conference on Energy, Power and Environment: Towards Clean Energy Technologies*, IEEE, Mar. 2021, pp. 1–6. doi: 10.1109/ICEPE50861.2021.9404390.
- [26] J. Richter and M. Doppelbauer, "Control and mitigation of current harmonics in inverter-fed permanent magnet synchronous machines with non-linear magnetics," *IET Power Electronics*, vol. 9, no. 10, pp. 2019–2026, Aug. 2016, doi: 10.1049/iet-pel.2015.0977.
- [27] Q. Salem, K. Alzaareer, and S. Harasis, "A performance comparison of series power flow control structures in a smart microgrid," *International Journal of Power Electronics and Drive Systems (IJPEDS)*, vol. 13, no. 2, pp. 908–917, Jun. 2022, doi: 10.11591/ijpeds.v13.i2.pp908-917.
- [28] L. F. J. Meloni, F. L. Tofoli, A. J. J. Rezek, and E. R. Ribeiro, "Modeling and experimental validation of a single-phase series active power filter for harmonic voltage reduction," *IEEE Access*, vol. 7, pp. 151971–151984, 2019, doi: 10.1109/ACCESS.2019.2947917.

BIOGRAPHIES OF AUTHORS



Ravikanth Mallajoshula    has received his B.Tech. degree in Electrical and Electronics Engineering in 2006 and M.E. degree in Industrial Drives & Control in 2013. Currently, he is pursuing Ph.D. degree in Electrical & Electronics engineering at "GITAM Deemed to be University", Visakhapatnam. His research interest includes power quality, grid connected systems, and power system. He can be contacted at email: ravikant235@gmail.com.



I. E. S. Naidu    has received his B.Tech. in Electrical and Electronics Engineering from JNTU, Hyderabad and M.Tech. in Advanced Power Systems from the JNTU, Kakinada in 2001 and 2005, respectively. He was awarded doctorate in Electrical Engineering by Andhra University in 2018. During 2005–2006, he worked with ANITS College and presently he is working as associate professor in Department of Electrical, Electronics and Communication Engineering, GITAM Deemed to be University, Visakhapatnam, India. His research interests include power system stability and power system security. He can be contacted at email: iesnaidu@gmail.com.